

## Structural Analysis of Alanine Tripeptide with Antiparallel and Parallel $\beta$ -Sheet Structures in Relation to the Analysis of Mixed $\beta$ -Sheet Structures in *Samia cynthia ricini* Silk Protein Fiber Using Solid-State NMR Spectroscopy

Tetsuo Asakura,\* Michi Okonogi, Yasumoto Nakazawa, and Kazuo Yamauchi

Contribution from the Department of Biotechnology, Tokyo University of Agriculture and Technology, 2-24-16 Nakacho, Koganei, Tokyo 184-8588, Japan

Received January 12, 2006; E-mail: asakura@cc.tuat.ac.jp

**Abstract:** The structural analysis of natural protein fibers with mixed parallel and antiparallel  $\beta$ -sheet structures by solid-state NMR is reported. To obtain NMR parameters that can characterize these  $\beta$ -sheet structures,  $^{13}\text{C}$  solid-state NMR experiments were performed on two alanine tripeptide samples: one with 100% parallel  $\beta$ -sheet structure and the other with 100% antiparallel  $\beta$ -sheet structure. All  $^{13}\text{C}$  resonances of the tripeptides could be assigned by a comparison of the methyl  $^{13}\text{C}$  resonances of Ala<sub>3</sub> with different [3- $^{13}\text{C}$ ]Ala labeling schemes and also by a series of RFDR (radio frequency driven recoupling) spectra observed by changing mixing times. Two  $^{13}\text{C}$  resonances observed for each Ala residue could be assigned to two nonequivalent molecules per unit cell. Differences in the  $^{13}\text{C}$  chemical shifts and  $^{13}\text{C}$  spin–lattice relaxation times ( $T_1$ ) were observed between the two  $\beta$ -sheet structures. Especially, about 3 times longer  $T_1$  values were obtained for parallel  $\beta$ -sheet structure as compared to those of antiparallel  $\beta$ -sheet structure, which could be explicable by the difference in the hydrogen-bond networks of both structures. This very large difference in  $T_1$  becomes a good measure to differentiate between parallel or antiparallel  $\beta$ -sheet structures. These differences in the NMR parameters found for the tripeptides may be applied to assign the parallel and antiparallel  $\beta$ -sheet  $^{13}\text{C}$  resonances in the asymmetric and broad methyl spectra of [3- $^{13}\text{C}$ ]Ala silk protein fiber of a wild silkworm, *Samia cynthia ricini*.

### Introduction

Silks are fibrous proteins with properties that intrigue scientists ranging from structural engineers to polymer chemists and biomedical researchers.<sup>1–3</sup> There are many kinds of silks produced by silkworms and spiders with a wide range of structures and properties.<sup>4</sup> Some silk fibers exhibit excellent mechanical properties such as high strength and high toughness.<sup>5</sup>

*Samia cynthia ricini* is a wild silkworm, and the amino acid composition of the silk fibroin is different from that of the silk fibroin from the domesticated silkworm, *Bombyx mori*.<sup>1</sup> The Gly and Ala residues are 82 mol %, which is similar to *B. mori* silk (71%), but the relative composition of Ala and Gly is reversed. The proportion of Gly residues is greater in *B. mori* silk fibroin, while the content of Ala residues is greater in *S.c. ricini* silk fibroin. The primary structure of *S.c. ricini* silk fibroin consists of similar sequences repeated about 100 times with alternative appearance of PLA (poly-L-alanine): (Ala)<sub>12–13</sub>

region and Gly-rich region.<sup>6</sup> The secondary structures of *S.c. ricini* silk fibroin before spinning have been studied with  $^{13}\text{C}$  solution NMR<sup>7–10</sup> and with  $^{13}\text{C}$  solid-state NMR.<sup>11–13</sup> The structural analysis at the atomic level of the appropriate model peptides, GGAGGGYGGDGG(A)<sub>12</sub>–GGAGDGYGAG, before spinning has been performed using several solid-state NMR methods, including  $^{13}\text{C}$  2D spin-diffusion solid-state NMR, rotational-echo double-resonance (REDOR) NMR, and the quantitative use of the conformation-dependent  $^{13}\text{C}$  CP/MAS chemical shifts.<sup>6,14</sup> After the spinning, it has been shown that *S.c. ricini* silk fiber took a  $\beta$ -sheet structure and the torsion angles of the backbone Ala and Gly residues were determined using  $^{13}\text{C}$  and  $^{15}\text{N}$  solid-state NMR<sup>12,15</sup> and the 2D DOQSY (correlation of the double-quantum and single-quantum spectra)

- (1) Asakura, T.; Kaplan, D. In *Encyclopedia of Agriculture Science*; Arutzen, C., Ed.; Academic Press: New York, 1994; Vol. 4, pp 1–11.
- (2) O'Brien, J.; Fahnestock, S.; Termonia, Y.; Gardner, K. *Adv. Mater.* **1998**, *10*, 1185–1195.
- (3) Altman, G.; Diaz, F.; Jakuba, C.; Calabro, T.; Horan, R.; Chen, J.; Lu, H.; Richmond, J.; Kaplan, D. *Biomaterials* **2003**, *24*, 401–416.
- (4) Vollrath, F.; Knight, D. In *Biopolymers*; Fahnestock, S., Steinbüchel, A., Eds.; Wiley-VCH: Weinheim, Germany, 2003; Vol. 8, pp 25–46.
- (5) Gosline, J.; Guerette, P.; Ortlepp, C.; Savage, K. *J. Exp. Biol.* **1999**, *202*, 3295–3303.

- (6) Nakazawa, Y.; Asakura, T. *J. Am. Chem. Soc.* **2003**, *125*, 7230–7237.
- (7) Asakura, T.; Murakami, T. *Macromolecules* **1985**, *18*, 2614–2619.
- (8) Asakura, T.; Kashiba, H.; Yoshimizu, H. *Macromolecules* **1988**, *21*, 644–648.
- (9) Nakazawa, Y.; Nakai, T.; Kameda, T.; Asakura, T. *Chem. Phys. Lett.* **1999**, *311*, 362–366.
- (10) Nakazawa, Y.; Asakura, T. *FEBS Lett.* **2002**, *529*, 188–192.
- (11) Saito, H.; Tabet, R.; Shoji, A.; Ozaki, T.; Ando, I. *Macromolecules* **1983**, *16*, 1050–1057.
- (12) Ishida, M.; Asakura, T.; Yokoi, M.; Saito, H. *Macromolecules* **1990**, *23*, 88–94.
- (13) van Beek, J.; Beaulieu, L.; Schafer, H.; Demura, M.; Asakura, T.; Meier, B. *Nature* **2000**, *405*, 1077–1079.
- (14) Nakazawa, Y.; Bamba, M.; Nishio, S.; Asakura, T. *Protein Sci.* **2003**, *12*, 666–671.
- (15) Asakura, T.; Ito, T.; Okudaira, M.; Kameda, T. *Macromolecules* **1999**, *32*, 4940–4946.

experiment.<sup>13</sup> The conformational change from  $\alpha$ -helix to  $\beta$ -sheet induced by stretching has been also monitored with <sup>13</sup>C solid-state NMR and MD (molecular dynamics) simulations.<sup>16</sup> During these studies, it was noticed that the  $\beta$ -sheet structure of *S.c. ricini* silk fiber or the 10 times stretched silk films of the fibroin is not as homogeneous as reported for *B. mori* silk fibroin fiber.<sup>17,18</sup> The sample inhomogeneity is clearly observed from the broad and asymmetric Ala methyl <sup>13</sup>C resonances in the <sup>13</sup>C CP/MAS NMR spectra of the *S.c. ricini* silk fiber. Such asymmetric Ala methyl <sup>13</sup>C resonances have been also observed in the <sup>13</sup>C CP/MAS NMR spectra of PLA with  $\beta$ -sheet structure<sup>11,19–21</sup> and silk-like proteins with  $\beta$ -sheet structures constructed from sequences of spider silk, *S.c. ricini*, and *B. mori* silk fibroins.<sup>22</sup> However, there are no other assignments. One possibility for the origin of such asymmetric Ala methyl <sup>13</sup>C resonances is the presence of both parallel and antiparallel  $\beta$ -sheet structures.

It has been found that the crystal structure of Alanine tripeptides, Ala–Ala–Ala (Ala<sub>3</sub>), grown from *N,N*-dimethylformamide (DMF)–water mixtures take 100% parallel and 100% antiparallel  $\beta$ -sheet structures by changing the solvent composition.<sup>23–25</sup> If the ratio by volume of DMF:H<sub>2</sub>O is 20:80 or less, the crystals grown by slow evaporation of solvent take an antiparallel  $\beta$ -sheet structure with one molecule of water of crystallization for every two Ala<sub>3</sub> molecules. In contrast, when the ratio by volume of DMF:H<sub>2</sub>O is more than 20:80, large platelets are obtained, which are found to have Ala<sub>3</sub> molecules in a parallel  $\beta$ -sheet structure, without any water molecules present in the crystal structure. Henceforth, Ala<sub>3</sub> molecules in the antiparallel  $\beta$ -sheet structure will be denoted AP-Ala<sub>3</sub>, and Ala<sub>3</sub> molecules in the parallel  $\beta$ -sheet structure will be denoted P-Ala<sub>3</sub>. The atomic coordinates of these two kinds of  $\beta$ -sheet structure have been reported with X-ray diffraction analysis. Thus, Ala<sub>3</sub> samples with parallel and antiparallel  $\beta$ -sheet structures are a suitable system to obtain characteristic NMR parameters for PLA with different  $\beta$ -sheet structure using solid-state NMR.

In this paper, solid-state NMR studies performed on alanine tripeptides with parallel and antiparallel  $\beta$ -sheet structures are reported to obtain characteristic NMR parameters for discussing the heterogeneous  $\beta$ -sheet structures of *S.c. ricini* silk fibroin fibers. The combination of the selective stable-isotope labeling of Ala<sub>3</sub> and the solid-state NMR techniques, <sup>13</sup>C CP/MAS NMR and RFDR (radio frequency driven recoupling),<sup>26,27</sup> was used for accurate spectral assignment and for obtaining information on intermolecular arrangements of Ala<sub>3</sub> molecules. Especially notable is the very large difference in the <sup>13</sup>C spin–lattice

**Table 1.** IR Frequencies of Ala<sub>3</sub> with Antiparallel  $\beta$ -Sheet and Parallel  $\beta$ -Sheet Structures<sup>25 a</sup>

band	characteristic absorptions (cm <sup>-1</sup> )	
	AP-structure	P-structure
amide I	1691MW, 1641VS, 1595W	1649VS, 1593VS
amide II	1547S, 1536S	1525S
amide III	1242sh, 1206VW	1344W, 1279M
amide IV	725W, 696VS, 687W	653W, 642VW, 631VS, 626VS, 618MW

<sup>a</sup> S, strong; M, medium; W, weak; V, very; sh, shoulder.

relaxation times of the methyl <sup>13</sup>C resonances of the parallel and antiparallel  $\beta$ -sheet structures of Ala<sub>3</sub>, which is extremely useful in the assignment of parallel and antiparallel  $\beta$ -sheet structures of *S.c. ricini* silk fibers.

## Materials and Methods

**Sample Preparation.** Singly <sup>13</sup>C-labeled samples [3-<sup>13</sup>C]Ala–Ala–Ala and Ala–Ala–[3-<sup>13</sup>C]Ala (<sup>13</sup>C: 99% enriched, Cambridge Isotopes Laboratories, Andover, MA) and uniformly <sup>13</sup>C-labeled Ala<sub>3</sub> (<sup>13</sup>C: 98% enriched) were manually synthesized by Fmoc solid-phase synthetic methods<sup>28</sup> and then purified by HPLC. The nonlabeled Ala<sub>3</sub> peptide was purchased from Bachem AG (Bubendorf, Switzerland).

Ala<sub>3</sub> samples with the AP- $\beta$ -sheet structure were prepared by dissolving in a minimal volume of H<sub>2</sub>O, and then dried in a rotary evaporator at 42 °C.<sup>23</sup> Ala<sub>3</sub> samples with the P- $\beta$ -sheet structure were obtained by dissolving in a minimal volume of 40% DMF, and after slow evaporation of H<sub>2</sub>O by the rotary evaporator, the tripeptide that precipitates in the remaining DMF was isolated by suction filtration.<sup>24</sup> In both cases, powder samples were obtained. The structures of all samples were confirmed by FT-IR, using the JASCO FT/IR-4100 instrument. The IR frequencies of Ala<sub>3</sub> with AP- and P-structures are listed in Table 1.

**<sup>13</sup>C CP/MAS NMR and <sup>13</sup>C T<sub>1</sub> Observation.** <sup>13</sup>C CP/MAS NMR spectra were obtained on a Chemagnetics Infinity 400 spectrometer at a frequency of 100.0 MHz for <sup>13</sup>C and 397.8 MHz for <sup>1</sup>H, using a Chemagnetics 4-mm HXY T-3 MAS probehead. A CP contact time of 1 ms, TPPM decoupling, MAS spinning speed of 7 kHz, and 70 kHz RF field was used during CP and decoupling. The sample used was about 40 mg for nonlabeled sample and 20 mg for labeled sample. A total of 1024 scans for nonlabeled samples and 160 scans for singly <sup>13</sup>C-labeled samples were collected over a spectral width of 35 kHz, with a recycle delay of 5 s. Chemical shifts were referenced to TMS using adamantane as a secondary standard (<sup>13</sup>CH peak at 28.8 ppm), and no line broadening was applied for processing the spectra. Deconvolution was performed with the MATLAB (MathWorks, Natick, MA) version 6.5.1. software. <sup>13</sup>C T<sub>1</sub> values of Ala methyl and methine carbons of Ala<sub>3</sub> with P- and AP- $\beta$ -sheet structures were obtained by the method of Torchia.<sup>29</sup> The area of deconvoluted peaks was used for the T<sub>1</sub> determination from a series of partially relaxed spectra.

**2D <sup>13</sup>C–<sup>13</sup>C RFDR NMR.** 2D <sup>13</sup>C–<sup>13</sup>C RFDR spectra were obtained on a Bruker DSX-400 AVANCE spectrometer operating at 100.4 MHz for <sup>13</sup>C and 399.3 MHz for <sup>1</sup>H, using a BL 4-mm Bruker MAS probe. The spectra were recorded according to a previously reported method with several modifications.<sup>27</sup> The MAS spinning speed was 15 kHz, and the CP contact time was set to 2 ms. Rotor-synchronized 180° pulses on <sup>13</sup>C with a length of 7.15  $\mu$ s and FSLG decoupling on <sup>1</sup>H at the rf field strength of 64 kHz were applied during the RFDR mixing time. The recycle delay was set to 3 s. A total of 512 t<sub>1</sub> acquisitions with 128 scans each were collected. The spectral width was 30 kHz in

(16) Yang, M.; Yao, J.; Sonoyama, M.; Asakura, T. *Macromolecules* **2004**, *37*, 3497–3504.

(17) Asakura, T.; Yao, J. *Protein Sci.* **2002**, *11*, 2706–2713.

(18) Asakura, T.; Yao, J.; Yamane, T.; Umemura, K.; Ulrich, A. *J. Am. Chem. Soc.* **2002**, *124*, 8794–8795.

(19) Lee, D.; Ramamoorthy, A. *J. Phys. Chem. B* **1999**, *103*, 271–275.

(20) Wildman, K.; Lee, D.; Ramamoorthy, A. *Biopolymers* **2002**, *64*, 246–254.

(21) Wildman, K.; Wilson, E.; Lee, D.; Ramamoorthy, A. *Solid State Nucl. Magn. Reson.* **2003**, *24*, 94–109.

(22) Yang, M.; Asakura, T. *J. Biochem.* **2005**, *137*, 721–729.

(23) Fawcett, J.; Camerman, N.; Camerman, A. *Acta Crystallogr.* **1975**, *B31*, 658–665.

(24) Hempel, A.; Camerman, N.; Camerman, A. *Biopolymers* **1991**, *31*, 187–192.

(25) Qian, W.; Bandekar, J.; Krimm, S. *Biopolymers* **1991**, *31*, 193–210.

(26) Bennett, A.; Ok, J.; Griffin, R.; Vega, S. *J. Chem. Phys.* **1992**, *96*, 8624–8627.

(27) Kono, H.; Numata, Y. *Polymer* **2004**, *45*, 4541–4547.

(28) Carpino, L. A.; Han, G. Y. *J. Am. Chem. Soc.* **1970**, *92*, 5748–5749.

(29) Torchia, D. A. *J. Magn. Reson.* **1978**, *30*, 613–616.

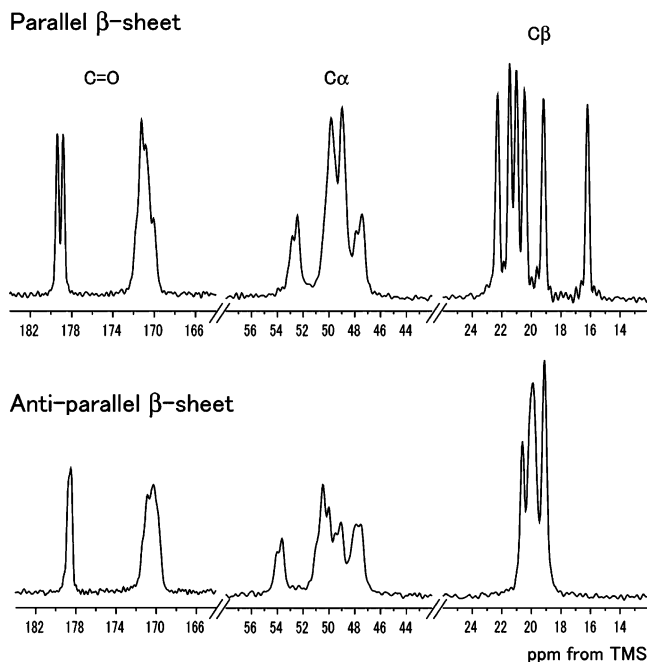


**Figure 1.**  $^{13}\text{C}$  CP/MAS NMR spectra of  $\text{Ala}_3$  with parallel  $\beta$ -sheet and antiparallel  $\beta$ -sheet structures.

both  $F_1$  and  $F_2$  dimensions. The mixing times were set to 15, 45, 90, 180, and 300 rotor cycles, which correspond to 1, 3, 6, 12, and 20 ms, respectively.

## Results

**$^{13}\text{C}$  CP/MAS NMR Spectra of  $\text{Ala}_3$  with P- and AP-Structures.** Figure 1 shows the  $^{13}\text{C}$  CP/MAS NMR spectra of  $\text{Ala}_3$  with parallel  $\beta$ -sheet (P-structure) and antiparallel  $\beta$ -sheet (AP-structure) structures. The spectra are considerably different between P- and AP-structures. There are six well-resolved  $C\beta$  peaks with equal intensity and equal full-width at half-maximum (fwhm) of about 30 Hz for  $\text{Ala}_3$  with P-structure. This indicates the presence of nonequivalent molecules. Actually, two nonequivalent A and B molecules per unit cell have been reported for  $\text{Ala}_3$  with P- and AP-structures with X-ray diffraction study.<sup>23,24</sup> The other  $^{13}\text{C}$  resonances split into more than three peaks due to the presence of nonequivalent molecules. The peak assignment for each residue was performed for Ala  $C\beta$  carbons from a comparison of the spectra of selectively  $^{13}\text{C}$ -labeled  $\text{Ala}_3$  peptides with different labeling positions. The assignment of each residue for P-structure is easily performed, as shown in Figure 2. The chemical shift differences between two nonequivalent molecules are larger at both terminal residues than the central residue. Contrary to the case of P-structure, the chemical shift range in the Ala  $C\beta$  peak is relatively small for  $\text{Ala}_3$  with AP-structure, and some peaks overlap. However, the peaks are also split due to the two nonequivalent molecules. The assignment of each residue was performed with selectively  $^{13}\text{C}$ -labeled peptides as shown in Figure 3. These data indicate that the difference in the electrostatic state around the Ala  $C\beta$  carbon between nonequivalent molecules is larger in the P-structure than in the AP-structure.

**RFDR Spectra of  $\text{Ala}_3$  with AP- and P-Structures.** Figure 4 shows a 2D  $^{13}\text{C}$ – $^{13}\text{C}$  RFDR spectrum of uniformly  $^{13}\text{C}$ -labeled  $\text{Ala}_3$  with the AP-structure with a mixing time of 1 ms. Three spectra in each figure are profiles of  $C\alpha$ – $C\beta$ ,  $C=O$ – $C\beta$ , and

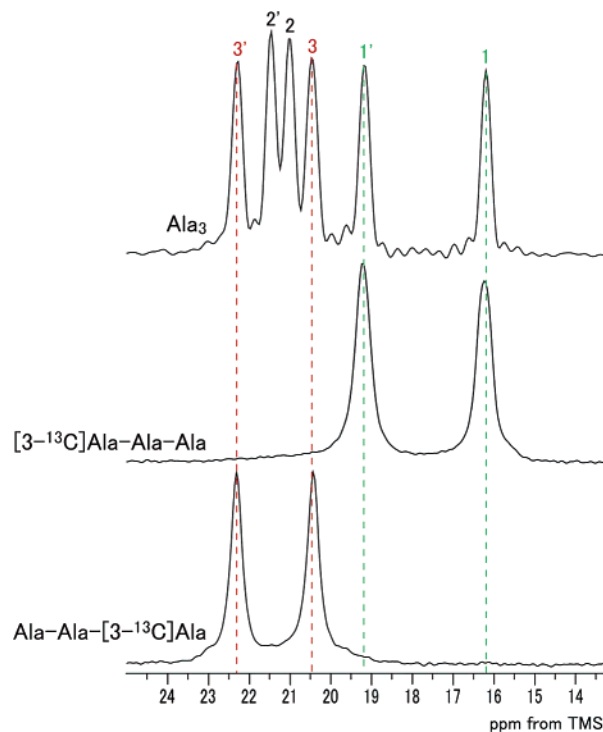


**Figure 2.** Expanded  $^{13}\text{C}$  CP/MAS NMR spectra of the  $C\beta$  region of  $\text{Ala}_3$ ,  $[3-^{13}\text{C}]\text{Ala-Ala-Ala}$ , and  $\text{Ala-Ala-[}^{13}\text{C}]\text{Ala}$  with parallel  $\beta$ -sheet structure. The lower field peak of each residue was noted with a dash on the number.

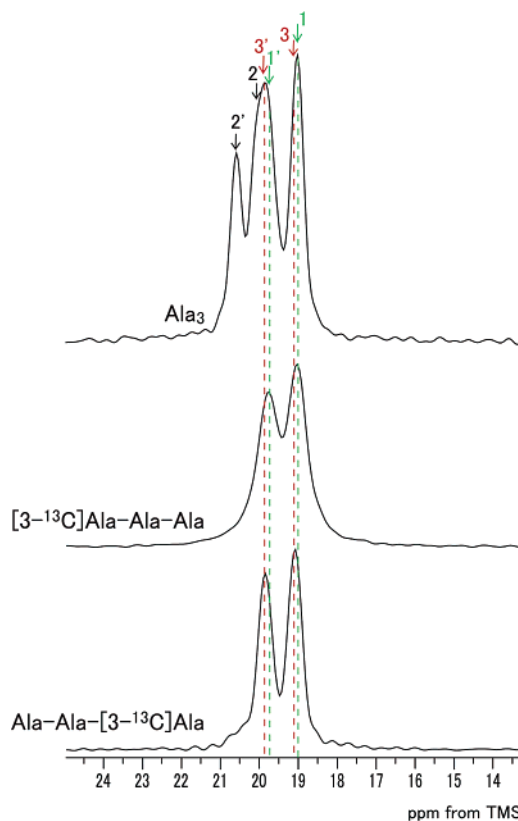


**Figure 3.** Expanded  $^{13}\text{C}$  CP/MAS NMR spectra of the  $C\beta$  region of  $\text{Ala}_3$ ,  $[3-^{13}\text{C}]\text{Ala-Ala-Ala}$ , and  $\text{Ala-Ala-[}^{13}\text{C}]\text{Ala}$  with antiparallel  $\beta$ -sheet structure. The lower field peak of each residue was noted with a dash on the number.

$\text{CO-C}\alpha$  cross-peaks correlation regions with 1D CP/MAS spectrum. Because of the presence of  $^{13}\text{C}$ – $^{13}\text{C}$  couplings, the  $^{13}\text{C}$  CP/MAS spectrum becomes broader, and therefore the  $^{13}\text{C}$

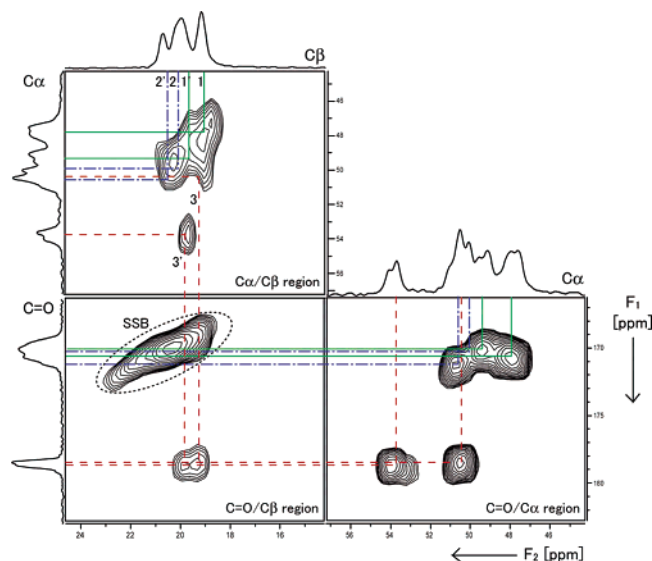


**Figure 4.** 2D  $^{13}\text{C}$ – $^{13}\text{C}$  RFDR spectrum of uniformly  $^{13}\text{C}$ -labeled AP-Ala<sub>3</sub> with a mixing time of 1 ms and at a MAS spinning speed of 15 kHz. The appropriate  $^{13}\text{C}$  CP/MAS spectra are shown on the vertical and horizontal lines. Numbers indicate the residue number, and the dashes indicate the lower field peak of the two  $C\beta$  peaks having the same residue number. SSB means spinning sidebands.

CP/MAS spectrum of nonlabeled Ala<sub>3</sub> is shown for tracing the peak position in Figure 4. Because the mixing time in the RFDR experiment is very short, 1 ms, only the short-range intraresidue  $^{13}\text{C}$ – $^{13}\text{C}$  coupling of the Ala<sub>3</sub> molecule could be observed. On the basis of Ala  $C\beta$  peak assigned to each carbon without assignment to A or B molecules, the assignment could be extended to Ala  $C\alpha$  and  $\text{C}=\text{O}$  carbons with the RFDR spectrum, although the correlation of  $\text{C}=\text{O}$ – $C\beta$  in the N-terminal and central residues could not be obtained because of overlapping of the peaks with the spinning sidebands. Nevertheless, using these correlations of intraresidue  $C\beta$ – $C\alpha$  and  $C\alpha$ – $\text{C}=\text{O}$ , six pairs of intraresidue assignments  $C\beta$ – $C\alpha$ – $\text{C}=\text{O}$  are obtained. Similarly, the assignment was also performed for Ala<sub>3</sub> with P-structure as shown in Figure 5.

**Assignments of Ala<sub>3</sub> Peaks to Interresidues and to Non-equivalent Molecules in the Unit Cell.** To obtain the correlation among Ala residues in one molecule or among Ala<sub>3</sub> molecules, the RFDR spectra were observed by changing mixing times: longer  $^{13}\text{C}$ – $^{13}\text{C}$  distance information will be obtained with increasing mixing time. Figure 6 shows a series of 2D  $^{13}\text{C}$ – $^{13}\text{C}$  RFDR spectra of uniformly  $^{13}\text{C}$ -labeled Ala<sub>3</sub> with the AP-structure for mixing times of 1, 3, 6, 12, and 20 ms. The  $\text{C}=\text{O}$ – $C\alpha$ ,  $\text{C}=\text{O}$ – $\text{C}=\text{O}$ ,  $C\alpha$ – $C\beta$ , and  $\text{C}=\text{O}$ – $C\beta$  regions are expanded. The three correlation peaks marked by the asterisk are newly observed in the former two regions by increasing the mixing times, indicating the correlations of the carbons among Ala residues in one molecule or among Ala<sub>3</sub> molecules. At first, we will discuss peak 3 (marked by red) in the  $\text{C}=\text{O}$ – $C\alpha$  region, which is observed only when the mixing time is 20 ms. The distance between the  $C\alpha$  carbon of the N-terminal Ala residue and  $\text{C}=\text{O}$  carbon of the C-terminal Ala residue within one molecule is longer than 8 Å from the X-ray diffraction data,<sup>23</sup> which is too long to observe in RFDR experiment. Therefore, the correlation, peak 3, should be observed between two carbons in different molecules. Actually, the shortest distance between the  $C\alpha$  carbon of the N-terminal Ala residue in A molecule

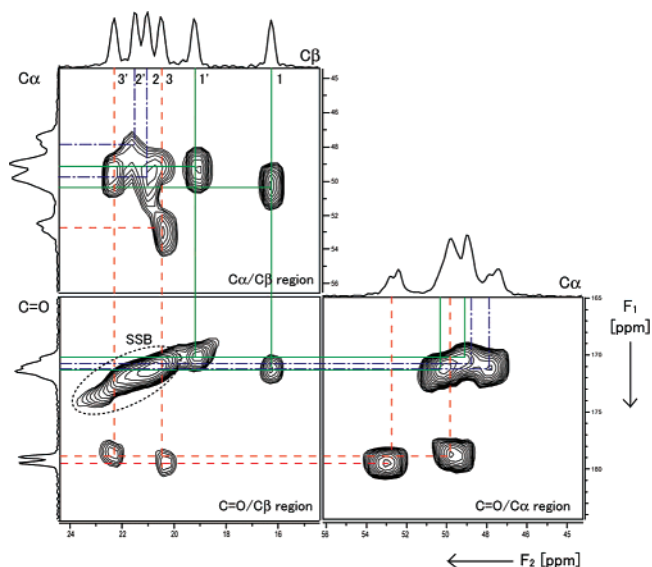


**Figure 5.** 2D  $^{13}\text{C}$ – $^{13}\text{C}$  RFDR spectrum of uniformly  $^{13}\text{C}$ -labeled P-Ala<sub>3</sub> with a mixing time of 1 ms and at a MAS spinning speed of 15 kHz. The appropriate  $^{13}\text{C}$  CP/MAS spectra are shown on the vertical and horizontal lines. Numbers indicate the residue number, and the dashes indicate the lower field peak of the two  $C\beta$  peaks having the same residue number. SSB means spinning sidebands.

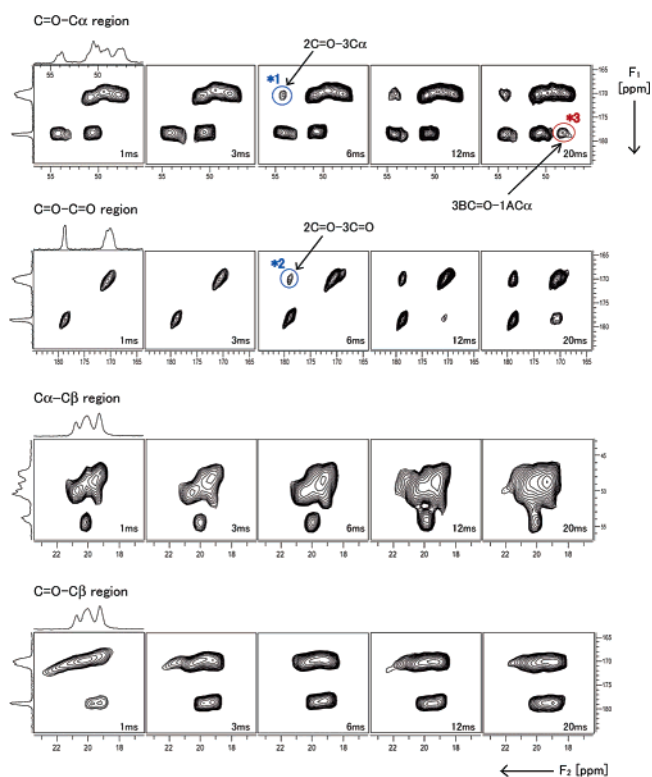


**Figure 6.** The series of extracted 2D  $^{13}\text{C}$ – $^{13}\text{C}$  RFDR spectra of uniformly  $^{13}\text{C}$ -labeled AP-Ala<sub>3</sub> recorded with different mixing times. Peaks \*1 and \*2 are cross-peaks representing intramolecular interresidue correlations, and peak \*3 is a cross-peak representing intermolecular interresidue correlations. Corresponding interatomic distances are illustrated in Figure 7.

and the  $\text{C}=\text{O}$  carbon of the C-terminal Ala residue in B molecule was reported to be 4.32 Å from the X-ray diffraction study,<sup>23</sup> as shown in Figure 7. Thus, the  $C\alpha$  peak at 47.9 ppm could be assigned to the N-terminal Ala residue in the A molecule and the  $\text{C}=\text{O}$  peak at 178.5 ppm to the C-terminal Ala residue in the B molecule.

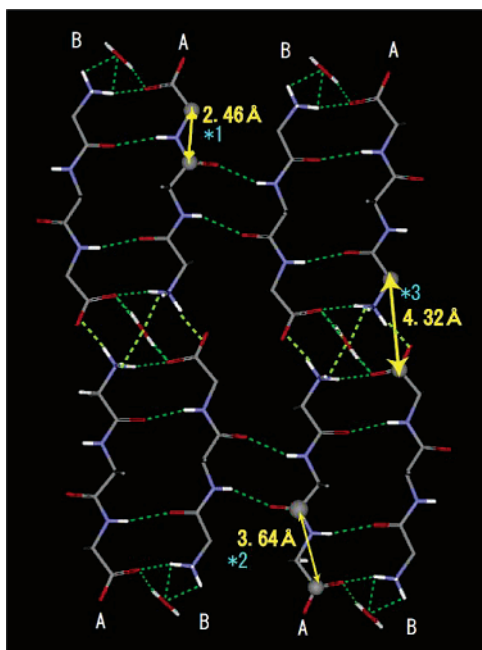


**Figure 7.** Interatomic distances corresponding to the marked peaks in Figure 6. These values were calculated from the model structure of Ala<sub>3</sub> with AP-structure, which was determined from X-ray diffraction analysis. The intermolecular hydrogen-bonding network was shown as broken lines. Distances \*1, \*2, and \*3 correspond to the peaks in Figure 6.

Contrary to peak 3, peaks 1 and 2 (marked by blue) in the C=O–C $\alpha$  and C=O–C=O regions, respectively, were observed when the mixing time was 6 ms. With increasing mixing times, the intensities become stronger. By reference of the distance information that peak 3 corresponds to 4.32 Å, these peaks can be assigned to the carbons with different residues within one molecule. As shown in Figure 7, peak 1 is assigned to the correlation between the C=O carbon of the central Ala residue and the C=O carbon of the C-terminal Ala residue in the same molecule. Although the distance of these carbons is almost the same between A and B molecules, the peaks are easily assigned to the A molecule judging from the chemical shift values and the assignment from peak 3 mentioned above. Similarly, peak 2 in the C=O–C=O region can be assigned to the correlation between the C=O carbon of the central Ala residue and the C=O carbon of the C-terminal Ala residue in A molecule. Thus, the peak assignments were performed for two nonequivalent A and B molecules per unit cell by change in the intensities of the cross-peaks as a function of mixing time by reference to the corresponding atomic distances of <sup>13</sup>C nuclei reported with X-ray diffraction analysis. The final assignments of Ala<sub>3</sub> with AP-structure are summarized in Table 2 together with the chemical shift values.

Figure 8 shows a series of 2D <sup>13</sup>C–<sup>13</sup>C RFDR spectra of uniformly <sup>13</sup>C-labeled Ala<sub>3</sub> with the P-structure recorded with mixing times of 1, 3, 6, 12, and 20 ms. The C=O–C $\alpha$ , C=O–C=O, C $\alpha$ –C $\beta$ , and C=O–C $\beta$  regions were also expanded. The five correlation peaks marked by the asterisk are newly observed by increasing the mixing times. By reference of the distance information on Ala<sub>3</sub> with the P-structure reported by X-ray diffraction study<sup>24</sup> (Figure 9), peaks 4 and 5 (marked by red) in the C=O–C $\beta$  region observed when the mixing time was 3 and 6 ms, respectively, can be assigned. Peak 4 can be assigned to the C=O carbon of the C-terminal Ala residue in

the A molecule and the C $\beta$  carbon of the N-terminal Ala residue in the B molecule because of the shortest distance of 3.97 Å obtained from the X-ray diffraction data. Similarly, peak 5 can be assigned to the correlation between the C=O carbon of the C-terminal Ala residue in the B molecule and the C $\beta$  carbon of the N-terminal Ala residue in the A molecule. Contrary to peaks 4 and 5, peaks 1–3 can be assigned to the carbons with different residues within one molecule by reference of X-ray diffraction data shown in Figure 9. The final assignments of Ala<sub>3</sub> with the P-structure are summarized in Table 2, together with the chemical shift values.

**<sup>13</sup>C Spin–Lattice Relaxation Times of Methyl and Methine Carbons of Ala<sub>3</sub> with P- and AP-Structures.** On the basis of the detailed peak assignments, <sup>13</sup>C spin–lattice relaxation times,  $T_1$ , are obtained for Ala<sub>3</sub> with the P- and AP-structures. Actually, the <sup>13</sup>C  $T_1$  values were very useful for assigning the asymmetric Ala methyl peaks of *B. mori* silk fibroin fiber where the main sequence is (AGSGAG)<sub>n</sub>.<sup>17,18</sup> Table 3 summarizes the <sup>13</sup>C  $T_1$  values for the methyl carbons of Ala<sub>3</sub> with two  $\beta$ -sheet structures. The  $T_1$  values of Ala methyl carbons change depending on the residue in the same molecule and also between the different A and B molecules. However, a large difference in  $T_1$  of Ala methyl carbon was observed between the P- and AP-structures; the  $T_1$  values of the P-structure are roughly 3 times longer than those of the AP-structure. For the main peak of the Ala methine carbon,  $T_1$  value was determined to be 7 s for the AP-structure and 19 s for the P-structure; a 2.7 times longer  $T_1$  value was also observed for P-structure similar to the case of Ala methyl  $T_1$ . Thus, a large difference in  $T_1$  between P- and AP-structures seems due to the difference in the backbone motion of Ala molecules between two structures. The  $T_1$  value may be a very good measure for differentiating between P- and AP-structures.

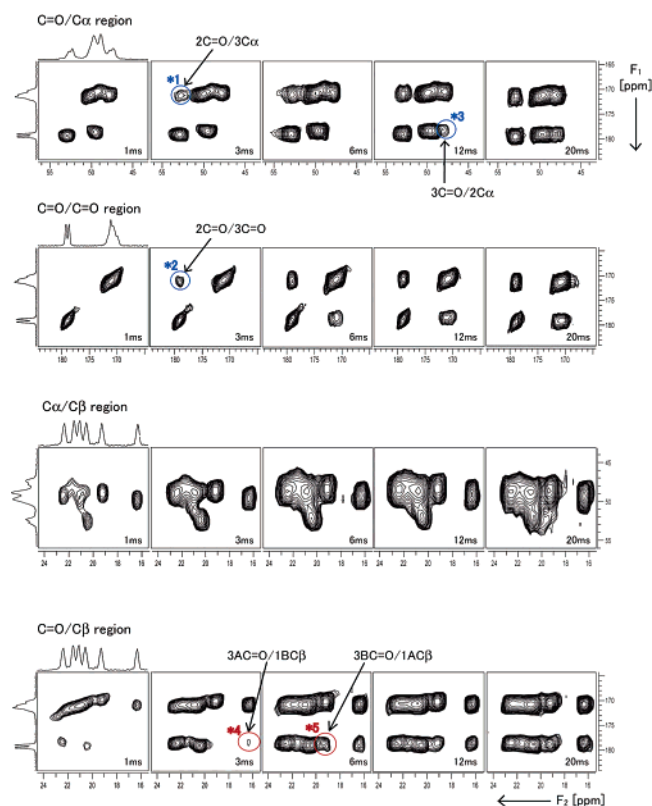
**<sup>13</sup>C Spin–Lattice Relaxation Times of Ala Methyl Carbon of [3-<sup>13</sup>C]Ala *S.c. ricini* Silk Fibroin Fiber.** Figure 10 shows the expanded Ala C $\beta$  region in the <sup>13</sup>C CP/MAS NMR spectrum of [3-<sup>13</sup>C]Ala *S.c. ricini* silk fibroin fiber, together with the chemical shifts, <sup>13</sup>C  $T_1$  values, and the fraction (%) of the resolved peaks. Judging from the conformation-dependent <sup>13</sup>C NMR chemical shifts of the Ala residue,<sup>16</sup> the broad peak (the fraction 12%) at 16.6 ppm can be assigned to random coil. The fraction of the isolated Ala residues in the Gly-rich region of *S.c. ricini* silk fibroin is approximately 10%, and therefore the 16.6 ppm peak seems to be assigned to such isolated Ala residues.<sup>6</sup> The other three peaks at the lower field can be assigned to  $\beta$ -sheet.

A series of the partially relaxed methyl peaks are shown in Figure 11. It is clear that the relaxation behavior of the lowest peak at 22.9 ppm is quite different from the others. The  $T_1$  values of the overlapping peaks at 19.8 and 21.2 ppm are almost the same, but the  $T_1$  value of the lowest field peak at 22.9 ppm is approximately 2 times longer. Thus, the lowest field peak can be assigned to parallel  $\beta$ -sheet structure and the overlapped peaks observed at higher field in the  $\beta$ -sheet region to antiparallel  $\beta$ -sheet judging from the  $T_1$  value. This is based on the large difference in  $T_1$  for methyl carbons of Ala<sub>3</sub> with P- and AP-structures described in the previous section.

Regarding the assignment of two peaks at 19.8 and 21.2 ppm, there are two possibilities; one is the difference in the torsion angles between two antiparallel  $\beta$ -sheet structures, and another

**Table 2.**  $^{13}\text{C}$  Chemical Shifts (ppm) of  $\text{Ala}_3$  with Antiparallel  $\beta$ -Sheet and Parallel  $\beta$ -Sheet Structures

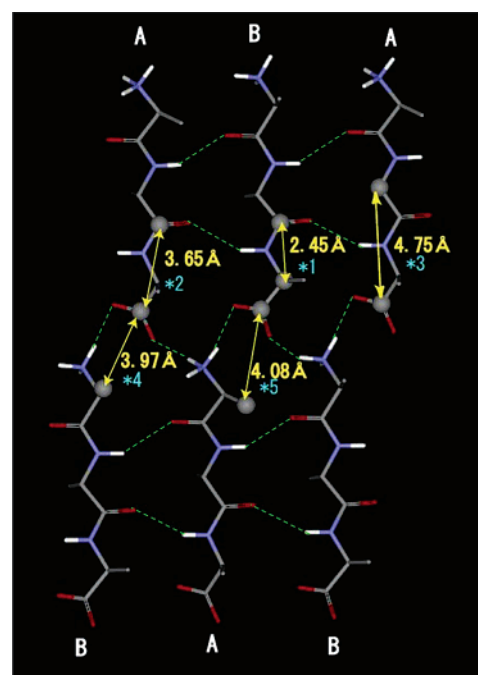
residue	AP-structure			P-structure		
	C=O	C $\alpha$	C $\beta$	C=O	C $\alpha$	C $\beta$
1A	170.7	47.9	19.0	170.1	49.1	19.2
1B	170.1	49.3	19.7	171.3	50.3	16.2
2A	171.1	50.6	20.6	171.2	47.9	21.5
2B	170.3	50.0	20.1	170.8	49.8	21.0
3A	178.7	53.8	19.9	178.8	49.8	22.3
3B	178.5	50.4	19.2	179.4	52.8	20.4

**Figure 8.** The series of extracted 2D  $^{13}\text{C}$ – $^{13}\text{C}$  RFDR spectra of uniformly  $^{13}\text{C}$ -labeled P- $\text{Ala}_3$  recorded with different mixing times. Peaks \*1, \*2, and \*3 are cross-peaks representing intramolecular interresidue correlations, and peaks \*4 and \*5 are cross-peaks representing intermolecular interresidue correlations. Corresponding interatomic distances are illustrated in Figure 9.

is the difference in the intermolecular chain arrangement. A further study on these two peaks will be required for the assignment.

## Discussion

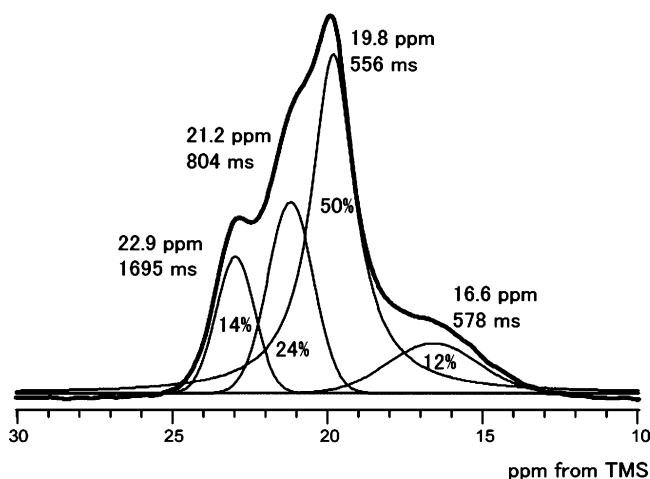
Detailed structural analysis of natural protein fiber is difficult because X-ray diffraction, used widely for the atomic level

**Figure 9.** Interatomic distances corresponding to the marked peaks in Figure 8. These values were calculated from the model structure of  $\text{Ala}_3$  with P-structure, which was determined from X-ray diffraction analysis. The intermolecular hydrogen-bonding network was shown as broken lines. Distances \*1–\*5 correspond to the peaks in Figure 8.

structure determination of protein single crystals, is not useful because of the limited number of diffraction data from the fiber samples. Thus, solid-state NMR has basically become the inherent merit for such fiber structure determination because solid-state NMR does not require single crystals. However, it is relatively difficult to analyze the intermolecular arrangement of the fiber molecules by solid-state NMR because this method gives relatively short-range structural information. It is also difficult to use solution NMR to characterize the fiber structure because of the insoluble character of the fiber. In this paper, we tried to characterize the structure of protein fibers with

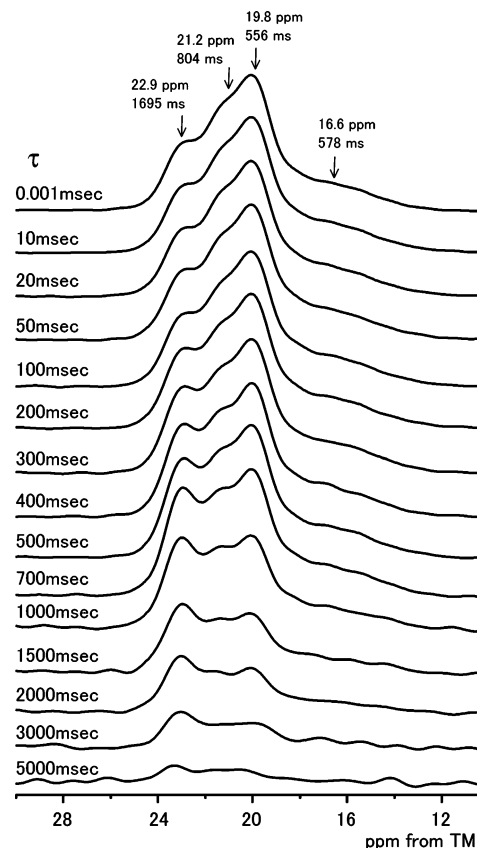
**Table 3.**  $^{13}\text{C}$   $T_1$  Relaxation Times of  $\text{C}\beta$  Peaks in  $\text{Ala}_3$  with Antiparallel  $\beta$ -Sheet and Parallel  $\beta$ -Sheet Structures

residue	AP-structure		P-structure	
	peak position (ppm)	carbon $T_1$ (ms)	peak position (ppm)	carbon $T_1$ (ms)
1A	19.0	123	19.2	296
1B	19.7	99	16.2	328
2A	20.6	168	21.5	397
2B	20.1	117	21.0	201
3A	19.9	75	22.3	682
3B	19.2	89	20.4	300

**Figure 10.** Expanded  $^{13}\text{C}$  CP/MAS NMR spectrum of the Ala  $\text{C}\beta$  region of  $[3\text{-}^{13}\text{C}]$  *S.c. ricini* silk fibroin fiber. The deconvoluted spectra are also shown, together with the chemical shifts,  $^{13}\text{C}$   $T_1$  values, and the fraction (%).

different intermolecular arrangements (mixed P- and AP- $\beta$ -sheet structures) using solid-state NMR. For this purpose, the structures of  $\text{Ala}_3$  with 100% P- or 100% AP- $\beta$ -sheet with known atomic coordinates were studied with  $^{13}\text{C}$  solid-state NMR to obtain characteristic NMR parameters for both  $\beta$ -sheet structures. The accurate  $^{13}\text{C}$  assignments, including two non-equivalent A and B molecules per unit cell, could be performed for  $\text{Ala}_3$  with  $[3\text{-}^{13}\text{C}]\text{Ala}$  labeling and RFDR experiments. The difference in the  $^{13}\text{C}$  chemical shift between two  $\beta$ -sheet structures is discussed. For example, the chemical shifts of 2A carbons are 20.6 and 21.5 ppm for AP- and P-structures, respectively. Similarly, the shifts are 20.1 and 21.0 ppm for AP- and P-structures, respectively, for 2B carbons. Thus, a 0.9 ppm lower field shift was observed for the methyl carbons in the central Ala residue, 2A and 2B, by changing the structure from AP- $\beta$ -sheet to P- $\beta$ -sheet. The torsion angles ( $\phi$  and  $\varphi$ ) of the central Ala residue with P-structure are reported as  $(-143.4^\circ, 160.2^\circ)$  for molecule A and  $(-164.1^\circ, 149.0^\circ)$  for molecule B.<sup>24</sup> For the AP-structure, the torsion angles ( $\phi$  and  $\varphi$ ) of the central Ala residue are reported as  $(-145.7^\circ, 145.5^\circ)$  for molecule A and  $(-156.2^\circ, 149.9^\circ)$  for molecule B.<sup>23</sup> Thus, the differences in torsion angles are within  $20^\circ$  between the two  $\beta$ -sheet structures, which means conformations similar to each other. Therefore, the chemical shift difference between the two  $\beta$ -sheet structures seems to be due to the difference in the electronic state reflecting the different intermolecular arrangement.

A more drastic difference between two structures is  $T_1$  values.  $^{13}\text{C}$   $T_1$  values were 3 times longer for the Ala  $\text{C}\alpha$  and  $\text{C}\beta$  carbons for the P- $\beta$ -sheet structure as compared to those of the AP- $\beta$ -sheet structure as summarized in Table 3. To interpret

**Figure 11.** A series of partially relaxed  $^{13}\text{C}$  NMR spectra of Ala  $\text{C}\beta$  peak of  $[3\text{-}^{13}\text{C}]$  *S.c. ricini* silk fibroin fiber as a function of the waiting time,  $\tau$ . Peaks from deconvolution are marked by arrows, and both the chemical shifts and the  $T_1$  values are shown.**Table 4.** Lengths ( $\text{\AA}$ ) and Angles (deg) for Hydrogen Bonds in  $\text{Ala}_3$  with Antiparallel  $\beta$ -Sheet and Parallel  $\beta$ -Sheet Structures<sup>a</sup>

	AP-structure		P-structure		
	donor– H···acceptor	D···A length ( $\text{\AA}$ )	D–H···A angle (deg)	donor– H···acceptor	D···A length ( $\text{\AA}$ )
N(2A)–H···O(2B)	2.918	158	N(2A)–H···O(1B)	3.204	148
N(2B)–H···O(2A)	2.915	158	N(3A)–H···O(2B)	3.200	156
N(3A)–H···O(1B)	2.988	160	N(2B)–H···O(1A)	3.363	134
N(3B)–H···O(1A)	3.066	162	N(3B)–H···O(2A)	3.349	149

<sup>a</sup> Here, the donor is peptide nitrogen.

the reason, the AP- and P-structures of  $\text{Ala}_3$  determined by X-ray diffraction analysis were examined carefully as shown in Figures 7 and 9.<sup>23,24</sup> In the P-structure, the Ala molecules are packed in parallel fashion with methyl groups alternately above and below the plane of the sheets and are held together in sheets by hydrogen bonds between carbonyl oxygen atoms and NH groups of neighboring molecules. Because of the parallel arrangement of molecules, there are only two hydrogen bonds between adjacent  $\text{Ala}_3$  molecules in sheets, as compared to an alternating series of four and two bonds in  $\text{Ala}_3$  with AP-structure where head-to-tail arrangement allows additional bonding between the zwitterionic terminal amino and carboxyl groups. In addition, the lengths and angles for hydrogen bonds in  $\text{Ala}_3$  with both  $\beta$  structures are listed in Table 4. These hydrogen bonds are weaker in quality as well in P-structure: the N···O distances and N–H···O angles average 3.28  $\text{\AA}$  and  $147^\circ$  versus 2.97  $\text{\AA}$  and  $160^\circ$  in the AP-structure. Thus, the large difference in  $T_1$  between the two  $\beta$ -sheet structures can be explained by the difference in these hydrogen-bonding networks. Such a loosely

packed P-structure enhances the backbone motion of Ala molecules as compared to the more tightly packed AP-structure, and this difference seems to be reflected in the  $T_1$  values of Ala C $\alpha$  and C $\beta$  carbons. The differences in the  $T_1$  values can be used for studying the heterogeneous  $\beta$ -sheet structure of silk protein fiber of a wild silkworm, *S.c. ricini*. As shown in Figure 10, judging from the  $T_1$  values, the lowest peak at 22.9 ppm is assigned to a P-structure and the overlapped two peaks at 19.8 and 21.2 ppm to an AP-structure. The lower field shift from AP- $\beta$ -sheet to P- $\beta$ -sheet is in the same direction as predicted from Ala<sub>3</sub> with both  $\beta$ -sheet structures, although the amount of the chemical shift difference is relatively small in the case of Ala<sub>3</sub>.

The <sup>13</sup>C CP/MAS NMR spectra of PLA with the length longer than 3 was examined from published papers. The spectra of Ala<sub>4</sub> and Ala<sub>5</sub> have been reported,<sup>20</sup> but the determination of atomic coordinates has not. The spectral patterns of both peptides are similar to each other and correspond to the pattern of Ala<sub>3</sub> with the AP-structure. Actually, we confirmed that Ala<sub>4</sub> sample that gives such a spectral pattern<sup>20</sup> takes on an AP-structure, judging from the FT-IR spectrum (Table 1). In addition, after methanol treatment of Ala<sub>4</sub> samples with AP-structure, we were able to convert the AP-structure to the P-structure. The <sup>13</sup>C CP/MAS NMR spectrum of Ala<sub>4</sub> with P-structure is quite similar to that of Ala<sub>3</sub> with P-structure; that is, the Ala C $\beta$  peak split into more than 5 peaks. These likely correspond to two nonequivalent molecules A and B, just as it was observed for Ala<sub>3</sub>. The  $T_1$  value of the Ala methyl peak of Ala<sub>4</sub> with AP-structure was approximately 100 ms, while the

$T_1$  value of the corresponding Ala methyl peak of Ala<sub>4</sub> with P-structure was 270–400 ms. Thus, <sup>13</sup>C  $T_1$  values are still roughly 3 times longer for the Ala C $\beta$  carbons for the P- $\beta$ -sheet structure as compared to those of the AP- $\beta$ -sheet structure. Further detailed structural and dynamical analyses of Ala<sub>4</sub> are now in progress.

In our previous paper,<sup>16</sup> the conformational transition,  $\alpha$ -helix to  $\beta$ -sheet, of *S.c. ricini* silk fibroin film induced by stretching was monitored by <sup>13</sup>C CP/MAS NMR. The resolved peaks at 20.8 and 22.8 ppm in the  $\beta$ -sheet region were observed when the stretching ratio was more than 6. Because of the relatively low-resolution spectrum, the peak at 20.8 ppm was considered a broad single peak and did not separate into two peaks (19.8 and 21.2 ppm). The relative intensities of these two peaks at 20.8 and 22.8 ppm increase with increasing stretching ratio from 6, 8, and 10, keeping the ratio of the fraction, roughly 1 (22.8 ppm peak):2 (20.8 ppm peak). This means that both structures, parallel and antiparallel  $\beta$ -sheet, appear when the  $\beta$ -sheet structure appears in *S.c. ricini* silk fibroin film by stretching.

Thus, the observed differences in these NMR parameters of Ala residue can be used to distinguish parallel or antiparallel  $\beta$ -sheet in peptides and proteins.

**Acknowledgment.** T.A. acknowledges support from the Insect Technology Project, Japan, and the Agriculture Biotechnology Project, Japan. We also thank Prof. Terry Gullion at West Virginia University for useful discussions.

JA060251T